

Age-Dependent Causal Effects of Mandibular Dose on Osteoradionecrosis Risk After Head and Neck Radiotherapy

Authors: Jingyuan Chen, PhD¹, Yunze Yang, PhD², Olivia M. Muller, MD³, Lei Zeng, MD¹, Zhengliang Liu, MS⁴, Tianming Liu, PhD⁴, Robert L. Foote, MD⁴, Daniel J. Ma, MD⁴, Samir H. Patel, MD¹, Zhong Liu, PhD^{6,*} and Wei Liu, PhD^{1,*}

¹Department of Radiation Oncology, Mayo Clinic, Phoenix, AZ 85054, USA

²Department of Radiation Oncology, the University of Miami, FL 33136, USA

³Department of Dental Specialties, Mayo Clinic Rochester, Rochester, MN, 55905, USA

⁴Department of Computer Science, University of Georgia, Athens, GA, 30602, USA

⁵, Mayo Clinic, Rochester, MN, 55905, USA

⁶Institute of Western China Economic Research, Southwestern University of Finance and Economics, Chengdu, Sichuan 611130, China

Co-Corresponding author: Wei Liu, PhD, Professor of Radiation Oncology, Department of Radiation Oncology, Mayo Clinic Arizona; e-mail: Liu.Wei@mayo.edu.

Conflicts of Interest Disclosure Statement

No

Funding Statement

This research was supported by NIH/NIBIB R01EB293388, by NIH/NCI R01CA280134, by the Eric & Wendy Schmidt Fund for AI Research & Innovation, and by the Kemper Marley Foundation.

Ethical Approval

This study was approved by Mayo Clinic Arizona institutional review board (IRB#: 24-011106).

Data Availability Statement

The data analyzed during the current study are not publicly available due to patient privacy concerns and institutional policies regarding protected health information (PHI). However, de-identified data that support the findings of this study are available from the corresponding author upon reasonable request and with appropriate institutional review board (IRB) approval.

Acknowledgments

This research was supported by NIH/BIBIB R01EB293388, by NIH/NCI R01CA280134, by the Eric & Wendy Schmidt Fund for AI Research & Innovation, and by the Kemper Marley Foundation.

Key Points

Question: How to quantify the causal effect of the dosimetric factors for osteoradionecrosis (ORN) of the mandible in patients with head and neck cancer treated with radiotherapy (RT)?

Findings: In this retrospective cohort study of 931 participants, all dosimetric factors (Dmax, Dmean, V40Gy, V50Gy, V60Gy) demonstrated positive causal effects on ORN development

with average treatment effects ranging from 0.092 to 0.141. Patients aged 50-60 years showed the strongest treatment effects

Meaning: The results suggest that dosimetric factors causally influence ORN risk with substantial heterogeneity across ages, illustrating the feasibility of causal analysis approaches in radiotherapy patient outcome studies.

Abstract

Importance: Mandibular osteoradionecrosis (ORN) is a serious late complication of head and neck radiotherapy, but the causal relationship between dosimetric factors and ORN incidence need to be identified and quantified.

Objective: To establish causal relationships between dosimetric factors and mandibular ORN using causal machine learning methods.

Design, Setting, and Participants: This retrospective cohort study analyzed consecutively treated, newly diagnosed head and neck cancer patients who received volumetric-modulated arc therapy (VMAT) at Anonymized Institution between April 2013 and August 2019. Eligible participants had conventional fractionation (120-220 cGy per fraction), prescription dose ≥ 60 Gy to high-risk targets, and >2 years of follow-up.

Exposure: Dosimetric parameters including maximum dose (Dmax), mean dose (Dmean), and dose-volume histogram indices (V40Gy, V50Gy, V60Gy) to the mandible during VMAT treatment, with clinical covariates including age, tumor stage, chemotherapy status, smoking status, diabetes status, and dental extraction.

Main Outcomes and Measures: Development of mandibular ORN identified through clinical examination, radiographic assessment, or pathologic confirmation. Causal effects were estimated using generalized random forest (GRF) to calculate average treatment effects (ATE) and

conditional average treatment effects (CATE). Clinical factor importance was assessed using SHAP (SHapley Additive exPlanations) values and GRF split-based importance.

Results: Of the 931 participants (mean age: 61 years), 46 (5%) developed mandibular ORN. All dosimetric factors showed positive average treatment effects: Dmean 0.134 (95% CI, 0.070-0.199), V40Gy 0.139 (95% CI, 0.072-0.207), V50Gy 0.135 (95% CI, 0.069-0.202), V60Gy 0.141 (95% CI, 0.057-0.224), and Dmax 0.092 (95% CI, 0.015-0.169). Age emerged as the most important clinical factor (GRF importance 44%, SHAP importance 39%). Conditional average treatment effect analysis revealed marked heterogeneity across age groups, with patients aged 50-60 years demonstrating the strongest treatment effects (CATE up to 0.229 for V50Gy), while those over 70 showed minimal effects (CATE 0.024-0.083). Robustness checks confirmed the validity of causal estimates.

Conclusions and Relevance: This study establishes causal relationships between dosimetric factors and mandibular ORN in head and neck cancer patients treated with VMAT, moving beyond traditional correlative analyses. The pronounced age-dependent heterogeneity in treatment effects, particularly the heightened vulnerability of patients aged 50-60 years, suggests that age-stratified treatment optimization and personalized treatment planning could reduce ORN risk.

Word Count of the Manuscript Main Text

2996 words

Introduction

Head and neck (H&N) cancer remains a major global health burden, ranking among the most common malignancies worldwide, with an estimated approximately 660,000 new cases and 325,000 deaths annually(1,2). Radiotherapy, particularly volumetric-modulated arc therapy (VMAT), is a cornerstone of H&N cancer management due to its high conformality and normal tissue sparing(3,4). Despite these technological advances, treatment-related adverse events (AEs) in H&N cancer remain substantial because tumors frequently abut - and may infiltrate - critical organs at risk (OARs) such as the mandible, salivary glands, larynx, pharyngeal constrictors, esophagus, and muscles of masticatory(5-8). Mandibular osteoradionecrosis (ORN) is among the most serious late toxicities after VMAT for H&N cancer(9,10). ORN involves radiation-induced injury to mandibular bone and surrounding tissues, leading to impaired healing, bone exposure, necrosis or fracture, chronic pain, trismus, and recurrent infection, all of which can markedly reduce quality of life and impose significant healthcare utilization.

Patient outcome study in radiotherapy is crucial to identifying risk factors, optimizing treatment protocols, and improving patient quality of life(6,9-17). For mandibular ORN specifically, multiple retrospective cohort studies have used statical analyses to identify dosimetric risk factors (such as, V50Gy, V60Gy, Dmax and Dmean) and corresponding threshold values(18-24). Several clinical factors (such as, preexisting dental disease, chemotherapy, smoking, diabetes) have also been associated with ORN incidence(20,21). More recently, artificial intelligence (AI) and machine learning approaches have been increasingly adopted in radiotherapy outcome prediction due to their ability to capture complex nonlinear relationships and achieve high predictive accuracy(25-30). However, the "black-box" nature of many AI models has limited their clinical adoption, prompting the development of explainable AI (XAI) techniques(31). Explainable machine learning

methods including SHAP (SHapley Additive exPlanations), LIME (Local Interpretable Model-agnostic Explanations), and attention mechanisms have been employed to enhance model interpretability while maintaining predictive performance(32-37).

To the best of our knowledge, nearly all patient-outcome studies in radiotherapy to date have been observational; consequently, their conclusions are correlational rather than causal. To formulate clinically actionable interventional recommendations, it is necessary to identify and estimate the causal effects of treatment factors such as dosimetric parameters on patient outcomes(38,39). Consider a familiar example, as shown in Fig.1(a): smoking increases the incidence of lung cancer and causes tooth discoloration. In observational data, tooth discoloration is therefore strongly associated with lung cancer; however, interventions targeting tooth discoloration (e.g., dental cleaning or whitening) would not reduce lung-cancer risk. Interventional recommendations derived solely from associations can be uninformative or even misleading.

Accordingly, rigorous causal quantification in patient-outcome research is essential. Traditional statistical approaches to analyzing radiation-induced toxicities have predominantly focused on correlative relationships rather than causal mechanisms, often struggling to disentangle the complex interplay between dosimetric and clinical factors. This limitation may lead to suboptimal treatment planning guidelines(38,39). Recent advances in causal inference methodology offer an opportunity to robustly identify factors that causally influence toxicity outcomes(38,40-43), rather than merely associate them.

In this retrospective cohort study, we integrate causal inference with explainable machine learning to analyze H&N cancer patients treated with VMAT at anonymized institution from 2013 to 2019.

The dataset includes mandibular ORN outcomes along with detailed dosimetric and clinical factors. Our objectives are: (i) to estimate the causal effects of dosimetric factors on the risk of ORN, and

(ii) to characterize the importance of clinical factors using interpretable learning methods. To our knowledge, this work is among the first in H&N radiotherapy to pair causal inference with model interpretability for late-toxicity research. By quantifying causal effects and elucidating key risk drivers, our findings aim to inform risk-adapted planning that reduces ORN while maintaining tumor control, ultimately improving patient quality of life.

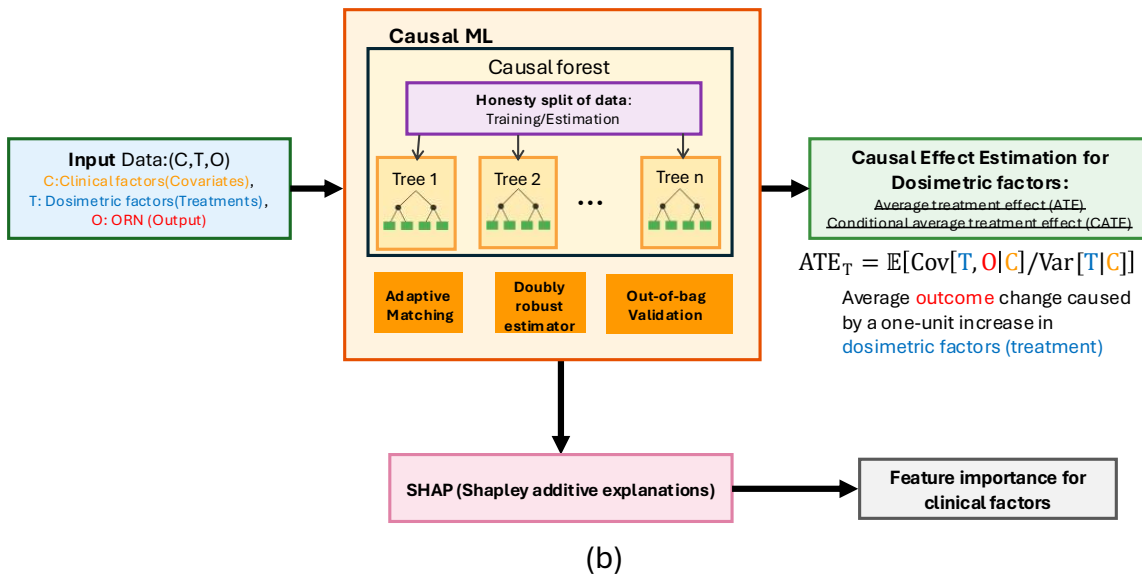
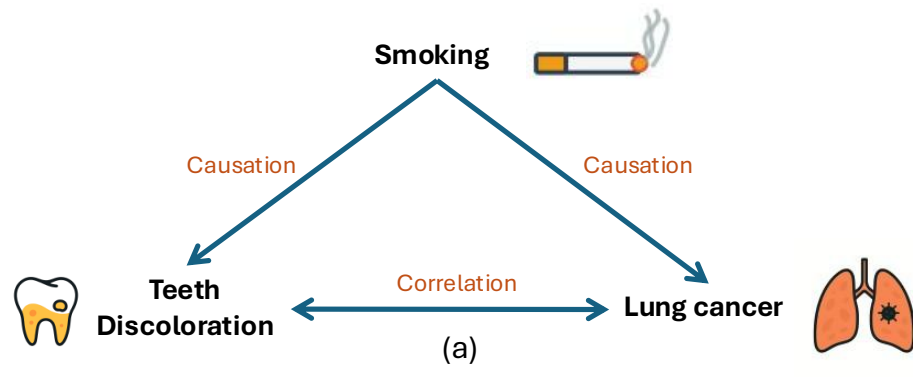


Figure.1 (a) Illustration of the difference between *causation* and *correlation*. While yellow teeth and lung cancer exhibit statistical correlation, this association is non-causal and we cannot give

interventional suggestions based on this correlation. Smoking acts as a common cause (confounding variable) that directly causes both yellow teeth and lung cancer. (b) The sketch of our approach for the causal analysis of the dosimetric factors and the importance analysis of the clinical factors. We employ the Causal Forest method, which is a tree-based causal machine learning method to reduce the bias from the real-word data and enable the estimation of the causal effects. The SHAP value and the importance based on the tree splitting frequency are adopted for the importance analysis of the clinical factors.

Methods and Materials

Patient Cohort

We included all consecutively treated, newly diagnosed head and neck (H&N) cancer patients at anonymized institutions A and B between April 2013 and August 2019 who received VMAT and had >2 years of follow-up, regardless of sex, age, minority status, vulnerable-population status, or body weight, and with a confirmed histologic diagnosis. The analytic dataset was restricted to patients who met all of the following criteria: (1) conventional fractionation of 120–220 cGy per fraction; (2) prescription dose ≥ 60 Gy to the high-risk target; and (3) for re-irradiated patients, negligible mandible dose on either the original or the re-treatment plan or documented ORN prior to re-irradiation. In total, 931 cases met these criteria. Demographic variables (e.g., age, sex) and relevant clinical information (e.g., prescription dose, tumor stage, concurrent chemotherapy, hypertension, diabetes, dental extraction, and smoking status [never, former, current]) were extracted (Supplemental Information [SI] Table 1). The study protocol was approved by the institutional review board (IRB). All patients granted permission to use their records for research purposes. The detailed information about diagnosis of ORN, treatment plans and dose calculation approaches are presented in the Supplementary Materials.

Causal Inference

In causal-effect analyses, patient-level variables are commonly grouped into three categories.

Treatment variables capture the exposure of interest, in this study, the dosimetric factors.

Covariates are factors that may influence treatment assignment, outcomes, or both; here, these

correspond to clinical factors. The **outcome** is the incidence of ORN. Our objective is to estimate treatment effects from observational data. We use the **Average Treatment Effect (ATE)** to quantify the population-level difference in potential outcomes under treatment versus no treatment.(42)

$$ATE = \mathbb{E}[O(T = 1) - O(T = 0)]$$

where $O(T = 1)$ and $O(T = 0)$ denote the potential outcomes, O , for the entire population under the treatment ($T = 1$) and control conditions ($T = 0$), respectively, T represents the treatment assignment. When the outcome is normalized and the treatment is binary, the ATE corresponds to the change in the probability of the outcome occurring when the treatment is applied versus when it is not applied.

Conditional average treatment effect for continuous variables

In cases where the treatment is continuous, such as dose, ATE represents the average outcome change caused by a one-unit increase in treatment variables:(44,45)

$$ATE = \mathbb{E} \left[\frac{Cov[T, O|C]}{Cov[T|C]} \right]$$

where $Cov[\cdot, \cdot]$ refers to covariance operator and C represents the covariates, which are the clinical factors. However, ATE only represents the populational causal effect. The Conditional Average Treatment Effect (CATE) extends beyond the population-level ATE by recognizing that treatments often affect different groups in distinct ways. (44,45)

$$CATE = \mathbb{E} \left[\frac{Cov[T, Y|C = c]}{Cov[T|C = c]} \right]$$

where $C=c$ represents conditioning on the specific subgroup characterized by clinical factors C taking value c . While the ATE provides a single summary measure of a treatment's impact across an entire population, CATE captures the heterogeneity in treatment responses by estimating the average effect within specific subgroups. By conditioning on covariates like age and tumor stage, CATE transcends one-size-fits-all conclusions to reveal specifically who benefits most from the intervention.

General random forest and robustness check

Our analysis employed causal forest (CF) methodology to quantify treatment effects, particularly focusing on ATE estimation(44-47). This approach adapts ensemble-based random forest techniques for causal analysis through the general random forest (GRF) framework, facilitating the identification of heterogeneous treatment responses across patient subgroups. The GRF algorithm constructs multiple decision trees; each trained on distinct data subsamples drawn without replacement. The splitting criterion at each node evaluates all possible partition points to optimize the separation of observations based on differential treatment responses. Notably, the algorithm prioritizes covariates that simultaneously influence both treatment assignment and outcomes, thereby addressing potential confounding effects from clinical factors. Out-of-bag validation was implemented to derive unbiased estimates of treatment effects and their standard errors, eliminating the need for separate validation datasets. This approach provided robust causal effect estimates for dosimetric parameters on ORN development while accounting for clinical variables. The details about robustness check are presented in the Supplementary Materials. Implementation was performed using the GRF package (version 2.4.0) in R statistical software

(version 4.4.1).

Clinical factor Importance

We adopt two approaches to characterize the importance of the clinical factors: Shapley additive explanations (SHAP) importance and the GRF split-based importance. We integrated GRF into SHAP algorithm to calculate feature importance for clinical factors(48). SHAP is a unified approach to explain the output of machine learning models based on game theory principles, specifically Shapley values. These values **quantify** each factor's contribution to the change in the expected model output when conditioning on that factor. The method is model-agnostic and maintains a strong theoretical foundation ensuring consistency. The SHAP value characterizes the correlation between the clinical factors and the patient outcomes.

The GRF split-based importance is defined as the weighted sum of how many times the clinical factor C was split on at each depth in the forest(47).

$$I_{GRF}(C) = \frac{S_{i=c}}{\sum_i S_i}$$

Where S_i represents the split times of the i th clinical factor and $S_{i=c}$ represents the split times of the specific clinical factor c . This importance measure captures the contribution of each clinical factor to the GRF model by tracking how frequently the factor is used to partition the data across all trees, with splits at shallower depths receiving higher weights to reflect their greater impact on the model. GRF split-based importance characterizes the contribution of the clinical factors to the heterogeneity of the treatment effects.

Following the global importance analysis, to investigate how individual clinical factors modulate

treatment effects, we generated SHAP dependence plots. The SHAP dependence plots visualize how the model's predictions change across the range of factor values (33,36,37,49). These plots reveal non-linear patterns and threshold effects that might not be apparent from population-level correlation analyses.

By combining GRF with SHAP values in our study, we were able to not only identify causal relationships between dosimetric factors but also quantify risky importance of clinical factor(50).

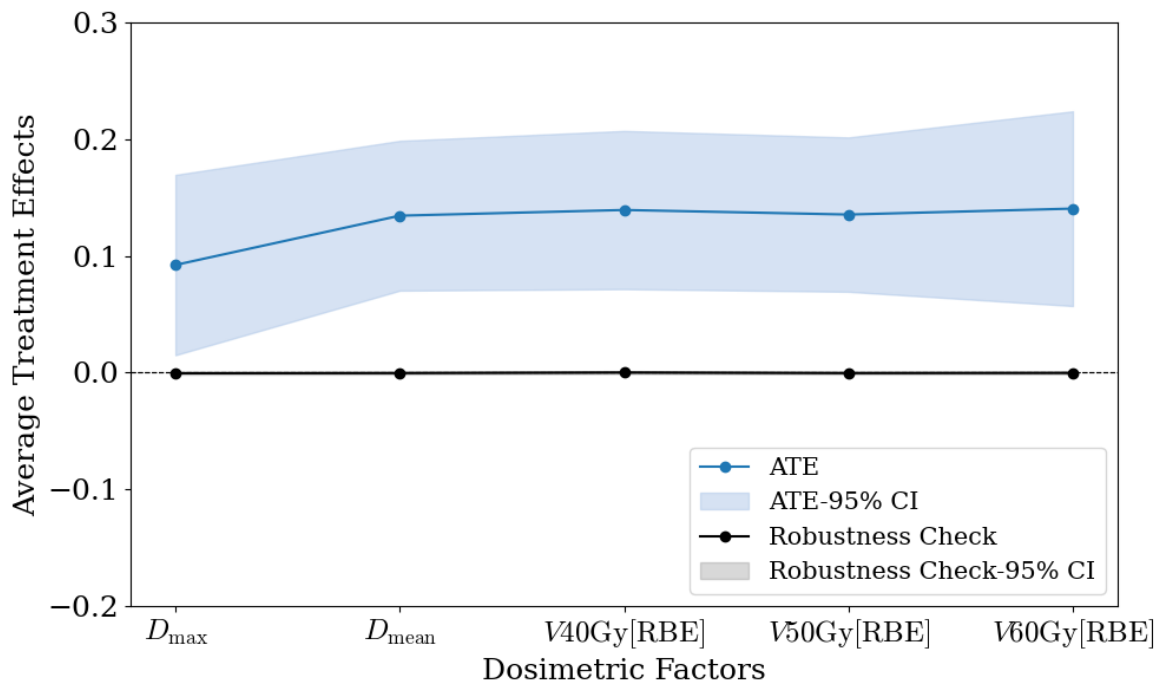


Figure 2. Average treatment effects of dosimetric factors obtained through the GRF method, with the method robustness check and 95% confidence intervals. The robustness check was calculated by replacing the actual data of each dosimetric factor with random numbers. Results closer to zero indicate greater robustness of the method.

Results

Average Treatment Effects of Dosimetric Factors

Figure 2 illustrates the ATEs of dosimetric factors obtained through the GRF method, with accompanying robustness validation. The analysis evaluated five key dosimetric parameters: maximum dose (Dmax), mean dose (Dmean), and three DVH indexes (V40Gy, V50Gy, and V60Gy). All dosimetric factors have positive ATE. Dmean, V40Gy, V50Gy, and V60Gy have a similar ATE. Dmean: 0.1344(95% CI: 0.0703–0.1986); V40Gy: 0.1393(95% CI: 0.0716-0.2071); V50Gy: 0.1354(95% CI: 0.0693-0.2015); V60Gy: 0.1405(95% CI: 0.0571-0.2239). The Dmax has the minimum ATE: 0.0922 (95% CI: 0.0150-0.1694).

The robustness check, displayed as the black horizontal line with gray confidence bands near zero, validated the reliability of our causal estimates. The absolute values of robustness check results are less than 0.001. When the actual dosimetric data were replaced with random numbers, the resulting effects converged to zero with narrow 95% confidence intervals, confirming that the observed treatment effects represent genuine causal relationships rather than methodological artifacts or chance findings. The clear separation between the actual ATEs and the robustness check results strengthens our confidence in the identified causal relationship.

These findings suggest that dosimetric factors, particularly Dmean, V40Gy, V50Gy, and V60Gy, have meaningful causal impacts on treatment outcomes.

Clinical Factor Importance and SHAP Analysis

The importances or the correlation between the clinical factors and ORN were quantified by two approaches: 1) SHAP values and 2) the split-based importance from the GRF model. The results are shown in Figure 3.

Both important scores agree that age is the most important clinical factor, with a GRF split-based importance of 44% and SHAP value of 39%. Diabetes was identified as the least correlated to ORN, with a GRF split-based importance of 2% and SHAP value of 2%. These two approaches also show agreements on tumor stage, smoking history, and chemotherapy.

Overall, SHAP value and GRF split-based importance show similar values for five of the eight clinical factors all of which are lower than age. These results underscore the critical need for further analysis about age.

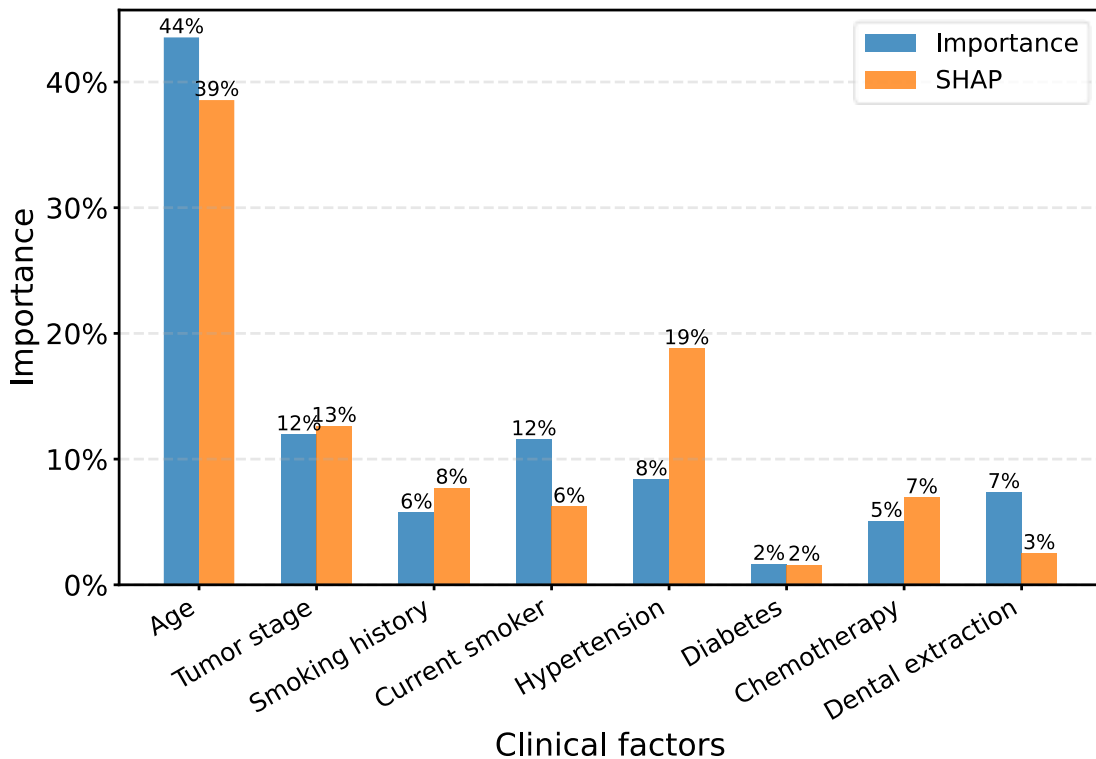


Figure 3. Importance of the clinical factors: The mean absolute SHAP value and the GRF split-based importance of the clinical factors. The SHAP value is obtained from the mean absolute values. The GRF split-based importance is based on how many times each clinical factor is split at each depth in the forest.

Age-Dependent SHAP Value Analysis

Figure 4 illustrates the SHAP value curve vs. age, revealing a distinctive non-linear relationship between patient age and treatment outcomes. The analysis demonstrates how age influences model predictions across the entire age spectrum, with individual patient data points (blue dots) showing the distribution of SHAP values at each age, and box plots summarizing the patterns for key age groups.

The SHAP values exhibit a clear inverted U-shaped relationship with age, characterized by three distinct phases. In the younger cohort (under 40 years), SHAP values remain lower value. A marked transition occurs in the 40-50 age group, where SHAP values increase substantially. The box plot for this cohort shows the highest SHAP value compared to other age subgroups, indicating the most significant correlation to the ORN incidence. Beyond age 60, a progressive decline in SHAP values is observed. The over-70 age group shows the lowest SHAP values. We should note that both SHAP value and GRF important score could only be interpreted as correlation instead of causation.

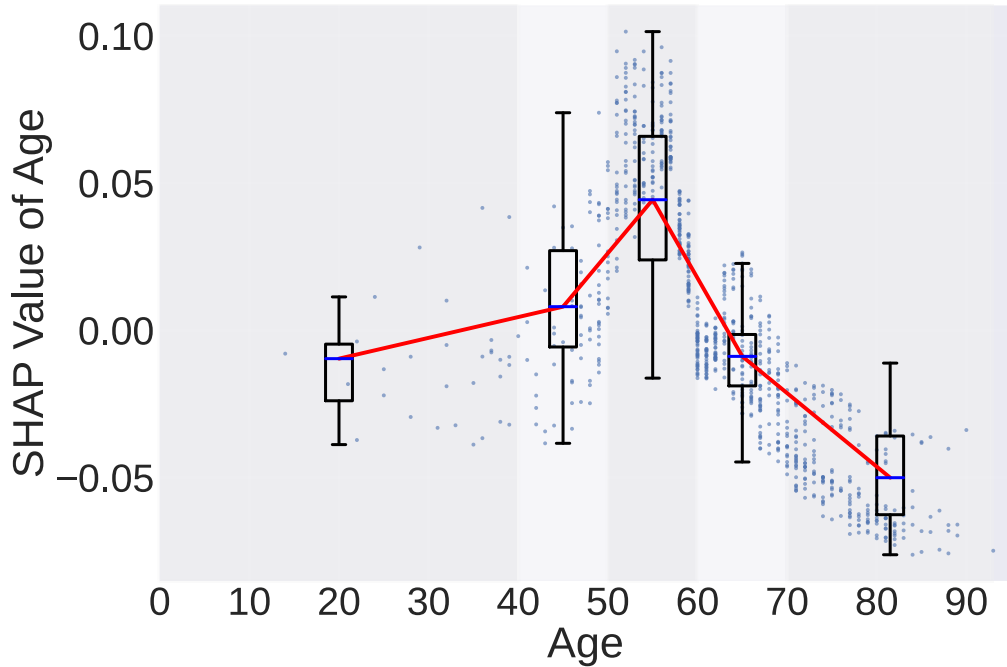


Figure 4. The SHAP value curve vs. Age. The blue points indicate SHAP value of each patient. The box plots are shown for the SHAP values of age in different age groups of under 40, 40-50, 50-60, 60-70, and over 70. Each box plot shows the interquartile range (IQR) with the median indicated by a blue line, whiskers extending to data points within $1.5 \times \text{IQR}$. The red line connects the median SHAP values across all boxes, revealing the trend of feature importance as the feature value changes.

Conditional Average Treatment Effects by Age Groups

Based on the significant importance of age, we calculated the CATE of different dosimetric factor in different age subgroups. Figure 5 presents the CATEs of different dosimetric factors stratified by age groups, revealing substantial heterogeneity in treatment effects across different age cohorts.

The analysis examines dosimetric indices of Dmax, Dmean, V40Gy, V50Gy, and V60Gy) across four age groups: under 50, 50-60, 60-70, and over 70 years. A striking age-dependent pattern emerges across all dosimetric factors. The 50-60 age group consistently demonstrates the strongest treatment effects, with CATEs of 0.1803 (95% CI: -0.0481, 0.4087) for Dmax to 0.2289 (95% CI: -0.0013, 0.3993) for V50Gy. The concentration of high CATE values in this age range corroborates our earlier SHAP value findings, confirming that patients in 50-60 age cohort derive the greatest benefit from reducing the mandible dose in the VMAT treatment.

The youngest cohort (under 50 years) and the 60-70 years cohort exhibit moderate treatment effects across most dosimetric factors. The elderly cohort (70+ years) shows the most attenuated treatment effects, with CATEs ranging from 0.0242 for Dmax (95% CI: -0.0273, 0.0757) to 0.0832 for V60Gy (95% CI: -0.0321, 0.1986). Across all subgroups, V60Gy has the largest treatment effect and Dmax has the lowest treatment effect, which agrees with the ATE result.

The confidence intervals for several estimates have negative values. The 95% CI and negative CATE of Dmax for the under 40 age group could be optimized by a larger cohort with more events. This reflects a limitation of causal ML approaches, which require larger volume data than conventional statistical analysis.

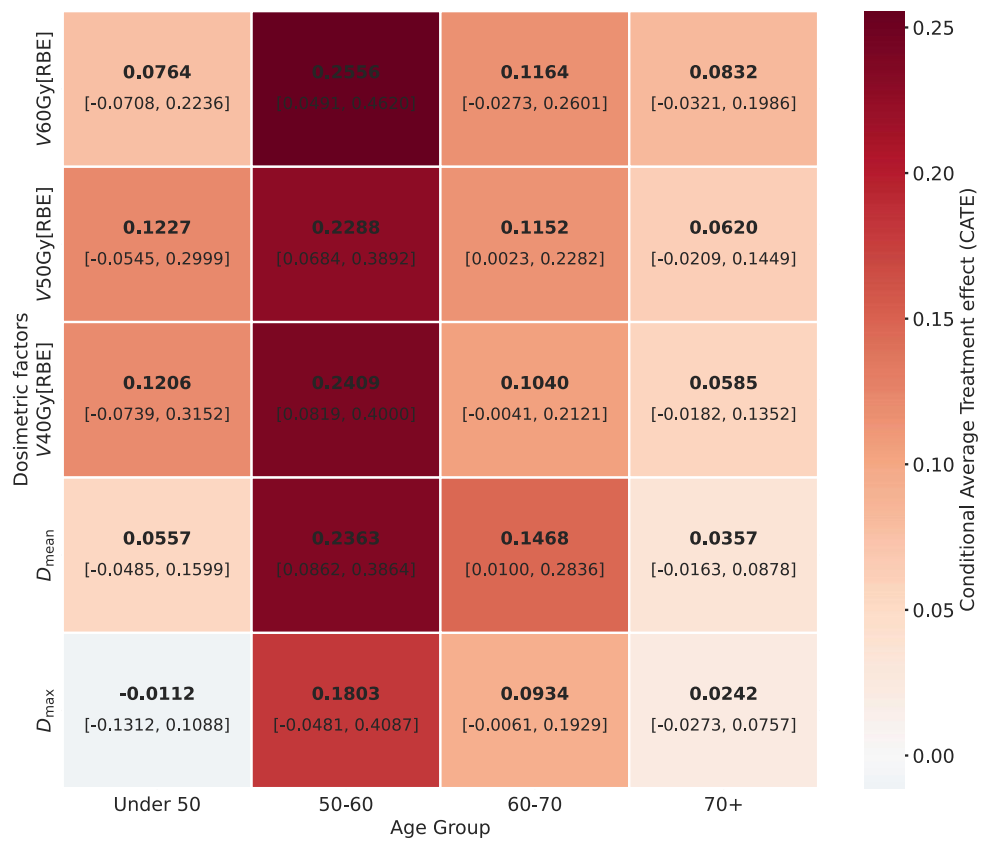


Figure 5. The conditional average treatment effect and 95% confidence intervals of the dosimetric factors D_{max} , D_{mean} , V40Gy, V50Gy and V60Gy by different age group. The ages are grouped by under 50, 50-60, 60-70 and over 70 years.

Discussion

To the best of our knowledge, this causal-based analysis represents the first combination of explainable machine learning and causal machine learning to quantitatively interpret the dosimetric and clinical factors in radiotherapy patient outcome study. Through the GRF method, we have quantified the causal relationship between dosimetric factors and ORN. We also identified age as the most important clinical factor associated with ORN. Through CATE and SHAP value analysis, our results suggest that for patients aged 50-60 years old, dosimetric indices demonstrate the most significant causal relationship with ORN development. Therefore, for this age group, optimizing mandibular dose during radiotherapy treatment planning warrant particular attention. Our study demonstrates the feasibility and value of causal machine learning approaches in analyzing radiotherapy patient outcomes, providing more viewpoints than traditional statistical methods.

We included 931 H&N cancer patients treated at our institution between 2013 and 2019 and the incidence rate of mandible ORN is found to be 5%. The important dosimetric factors and known clinical factors possibly related to mandible ORN are included in the study. Based on this large and comprehensive retrospective dataset and the novel causal ML methodology, we successfully quantify the causal relationship between dosimetric factors and ORN. All dosimetric factors showed positive ATEs, confirming their causal relationship with ORN. V40Gy, V50Gy, V60Gy and Dmean shows the comparable ATE, while Dmax shows less causal relationship with ORN. This suggests that the mean dose and the intermediate doses of mandible are more important than the maximum dose in respect to minimizing the incidence rates of ORN, which agrees with the reported results(11,18,51-55).

Another important innovation of our work is to demonstrate the feasibility of using causal methods

to provide evidence for personalized treatment plans in radiotherapy. We creatively integrate causal machine learning with explainable machine learning to produce importance rankings for clinical factors. We stratified the most important clinical factor, age, and then further computed the CATE of dosimetric factors of different age groups for ORN. Our results show that, within the 50–60 age group, various dosimetric factors have a more pronounced causal effect on the occurrence of ORN; this is consistent with and explains the SHAP value curve vs. age derived from the explainable machine learning.

A key point of interpretation is the distinction between importance, causation, and association for clinical factors. Clinical factor importance related to SHAP values derived from explainable machine learning methods should be understood as evidence of a strong statistical association between age and ORN—not as a proof that age *causes* ORN. Our subsequent CATE analysis further clarifies this distinction: the strong association observed for the 50–60-year subgroup with ORN arises because, within this age range, dosimetric factors have stronger *causal* effects on ORN. This underscores the necessity of employing causal machine-learning approaches to quantify causal effects rather than relying on association-based SHAP value alone derived from explainable machine learning methods.

Limitations

Despite the valuable insights gained, several limitations warrant consideration. First, causal machine learning approaches typically require substantially larger data volumes, and our relatively small sample size resulted in wider 95% confidence intervals. Second, while we endeavored to satisfy the three key assumptions of causal inference (independence, ignitability, and positivity), achieving complete fulfillment would require even more comprehensive clinical databases. Given

that ORN is a late-occurring complication, study with longer follow-up might provide more definitive results. Finally, while our approach represents methodological advancement, prospective validation in independent patient cohorts would further strengthen our findings.

Conclusion

This study pioneers the integration of causal machine learning with explainable machine learning to establish causal relationships between dosimetric factors and mandibular ORN in 931 H&N cancer patients treated with VMAT. Our analysis advances beyond traditional correlative studies to provide actionable causal evidence for treatment optimization. Key findings include significant causal effects of dosimetric indices on ORN development (ATE: 0.09-0.14), with marked heterogeneity across age groups. Patients aged 50-60 years demonstrated the strongest treatment effects (CATE >0.22 for dosimetric indices), while those over 70 showed minimal response, indicating the need to further explore the concept of using age to further personalize treatment planning in radiotherapy.

References

1. Gormley M, Creaney G, Schache A, et al. Reviewing the epidemiology of head and neck cancer: Definitions, trends and risk factors. *Br Dent J* 2022;233:780-786.
2. Bray F, Laversanne M, Sung H, et al. Global cancer statistics 2022: Globocan estimates of incidence and mortality worldwide for 36 cancers in 185 countries. *CA: A Cancer Journal for Clinicians* 2024;74:229-263.
3. Otto K. Volumetric modulated arc therapy: Imrt in a single gantry arc. *Medical Physics* 2008;35:310-317.
4. Teoh M, Clark CH, Wood K, et al. Volumetric modulated arc therapy: A review of current literature and clinical use in practice. *British Journal of Radiology* 2011;84:967-996.
5. Machtay M, Moughan J, Trott A, et al. Factors associated with severe late toxicity after concurrent chemoradiation for locally advanced head and neck cancer: An rtog analysis. *Journal of Clinical Oncology* 2008;26:3582-3589.
6. Chen J, Yang Y, Liu C, et al. Critical review of patient outcome study in head and neck cancer radiotherapy. *Meta-Radiology* 2025;3:100151.
7. Dornfeld K, Simmons JR, Karnell L, et al. Radiation doses to structures within and adjacent to the larynx are correlated with long-term diet- and speech-related quality of life. *Int J Radiat Oncol Biol Phys* 2007;68:750-7.
8. Eisbruch A, Schwartz M, Rasch C, et al. Dysphagia and aspiration after chemoradiotherapy for head-and-neck cancer: Which anatomic structures are affected and can they be spared by imrt? *Int J Radiat Oncol Biol Phys* 2004;60:1425-39.
9. Singh A, Kitpanit S, Neal B, et al. Osteoradionecrosis of the jaw following proton radiation therapy for patients with head and neck cancer. *JAMA Otolaryngology-Head & Neck Surgery* 2023;149:151-159.
10. Topkan E, Kucuk A, Somay E, et al. Review of osteoradionecrosis of the jaw: Radiotherapy modality, technique, and dose as risk factors. *J Clin Med* 2023;12.
11. Aarup-Kristensen S, Hansen CR, Forner L, et al. Osteoradionecrosis of the mandible after radiotherapy for head and neck cancer: Risk factors and dose-volume correlations. *Acta Oncol* 2019;58:1373-1377.
12. Lee IJ, Koom WS, Lee CG, et al. Risk factors and dose-effect relationship for mandibular osteoradionecrosis in oral and oropharyngeal cancer patients. *Int J Radiat Oncol Biol Phys* 2009;75:1084-91.
13. Luo Y, Chen S, Valdes G. Machine learning for radiation outcome modeling and prediction. *Med Phys* 2020;47:e178-e184.
14. Yang Y, Muller OM, Schild SE, et al. Empirical relative biological effectiveness (rbe) for mandible osteoradionecrosis (orn) in head and neck cancer patients treated with pencil-beam-scanning proton therapy (pbspt): A retrospective, case-matched cohort study. *Frontiers in Oncology* 2022;12:843175.
15. Diamant A, Chatterjee A, Vallières M, et al. Deep learning in head & neck cancer outcome prediction. *Scientific reports* 2019;9:2764.
16. Hu J, Schild S, Liu W, et al. Improving dose volume histogram (dvh) based analysis of clinical outcomes using modern statistical techniques: A systematic answer to multiple comparisons concerns. *International Journal of Radiation Oncology, Biology, Physics* 117(2), S 2023;20.

17. Peterson DE, Koyfman SA, Yarom N, et al. Prevention and management of osteoradionecrosis in patients with head and neck cancer treated with radiation therapy: Isso-mascc-asco guideline. *Journal of Clinical Oncology* 2024;42:1975-1996.
18. Caparrotti F, Huang SH, Lu L, et al. Osteoradionecrosis of the mandible in patients with oropharyngeal carcinoma treated with intensity-modulated radiotherapy. *Cancer* 2017;123:3691-3700.
19. Mohamed ASR, Hobbs BP, Hutcheson KA, et al. Dose-volume correlates of mandibular osteoradionecrosis in oropharynx cancer patients receiving intensity-modulated radiotherapy: Results from a case-matched comparison. *Radiotherapy and Oncology* 2017;124:232-239.
20. Lang K, Held T, Meixner E, et al. Frequency of osteoradionecrosis of the lower jaw after radiotherapy of oral cancer patients correlated with dosimetric parameters and other risk factors. *Head & Face Medicine* 2022;18:7.
21. Kubota H, Miyawaki D, Mukumoto N, et al. Risk factors for osteoradionecrosis of the jaw in patients with head and neck squamous cell carcinoma. *Radiation Oncology* 2021;16:1.
22. Tsai CJ, Hofstede TM, Sturgis EM, et al. Osteoradionecrosis and radiation dose to the mandible in patients with oropharyngeal cancer. *International Journal of Radiation Oncology* Biology* Physics* 2013;85:415-420.
23. Treechairusame T, Singh A, Dee EC, et al. Osteoradionecrosis as a complication following post-operative intensity-modulated radiation therapy or proton therapy for oral cavity cancer. *Oral Oncology* 2025;168:107581.
24. Möring MM, Mast H, Wolvius EB, et al. Osteoradionecrosis after postoperative radiotherapy for oral cavity cancer: A retrospective cohort study. *Oral Oncology* 2022;133:106056.
25. Kang J, Schwartz R, Flickinger J, et al. Machine learning approaches for predicting radiation therapy outcomes: A clinician's perspective. *International Journal of Radiation Oncology*Biology*Physics* 2015;93:1127-1135.
26. Dean JA, Wong KH, Welsh LC, et al. Normal tissue complication probability (ntcp) modelling using spatial dose metrics and machine learning methods for severe acute oral mucositis resulting from head and neck radiotherapy. *Radiotherapy and Oncology* 2016;120:21-27.
27. Humbert-Vidan L, Patel V, Oksuz I, et al. Comparison of machine learning methods for prediction of osteoradionecrosis incidence in patients with head and neck cancer. *British Journal of Radiology* 2021;94:20200026.
28. Reber B, Van Dijk L, Anderson B, et al. Comparison of machine-learning and deep-learning methods for the prediction of osteoradionecrosis resulting from head and neck cancer radiation therapy. *Advances in Radiation Oncology* 2023;8:101163.
29. Zhen X, Chen J, Zhong Z, et al. Deep convolutional neural network with transfer learning for rectum toxicity prediction in cervical cancer radiotherapy: A feasibility study. *Physics in Medicine & Biology* 2017;62:8246.
30. Sheikh K, Lee SH, Cheng Z, et al. Predicting acute radiation induced xerostomia in head and neck cancer using mr and ct radiomics of parotid and submandibular glands. *Radiation Oncology* 2019;14:131.
31. Lundberg SM, Lee S-I. A unified approach to interpreting model predictions. *Advances in neural information processing systems* 2017;30.
32. Tjoa E, Guan C. A survey on explainable artificial intelligence (xai): Toward medical xai. *IEEE Transactions on Neural Networks and Learning Systems* 2021;32:4793-4813.
33. Lundberg SM, Nair B, Vavilala MS, et al. Explainable machine-learning predictions for the prevention of hypoxaemia during surgery. *Nature Biomedical Engineering* 2018;2:749-760.

34. Ribeiro MT, Singh S, Guestrin C. "Why should i trust you?": Explaining the predictions of any classifier. In: Editor, editor^editors. Book "Why should i trust you?": Explaining the predictions of any classifier. San Francisco, California, USA: Association for Computing Machinery; 2016. pp. 1135–1144.

35. Selvaraju RR, Cogswell M, Das A, et al. Grad-cam: Visual explanations from deep networks via gradient-based localization. Proceedings of the IEEE international conference on computer vision. 2017. pp. 618–626.

36. Lee SH, Geng H, Arnold J, et al. Interpretable machine learning for choosing radiation dose-volume constraints on cardio-pulmonary substructures associated with overall survival in nrg oncology rtog 0617. *Int J Radiat Oncol Biol Phys* 2023;117:1270-1286.

37. Lauritsen SM, Kristensen M, Olsen MV, et al. Explainable artificial intelligence model to predict acute critical illness from electronic health records. *Nat Commun* 2020;11:3852.

38. Prosperi M, Guo Y, Sperrin M, et al. Causal inference and counterfactual prediction in machine learning for actionable healthcare. *Nature Machine Intelligence* 2020;2:369–375.

39. Feuerriegel S, Frauen D, Melnychuk V, et al. Causal machine learning for predicting treatment outcomes. *Nat Med* 2024;30:958–968.

40. Imai K, Van Dyk DA. Causal inference with general treatment regimes: Generalizing the propensity score. *Journal of the American Statistical Association* 2004;99:854–866.

41. Rubin DB. Causal inference using potential outcomes: Design, modeling, decisions. *Journal of the American Statistical Association* 2005;100:322–331.

42. Yao L, Chu Z, Li S, et al. A survey on causal inference. *ACM Transactions on Knowledge Discovery from Data* 2021;15:1–46.

43. Nie L, Ye M, Liu Q, et al. Vcnet and functional targeted regularization for learning causal effects of continuous treatments. *arXiv preprint arXiv:210307861* 2021.

44. Wager S, Athey S. Estimation and inference of heterogeneous treatment effects using random forests. *Journal of the American Statistical Association* 2018;113:1228–1242.

45. Sverdrup E, Petukhova M, Wager S. Estimating treatment effect heterogeneity in psychiatry: A review and tutorial with causal forests. *International Journal of Methods in Psychiatric Research* 2025;34:e70015.

46. Athey S, Wager S. Estimating treatment effects with causal forests: An application. *Observational studies* 2019;5:37–51.

47. Athey S, Tibshirani J, Wager S. Generalized random forests 2019.

48. Lundberg SM, Erion G, Chen H, et al. From local explanations to global understanding with explainable ai for trees. *Nature Machine Intelligence* 2020;2:56–67.

49. Nohara Y, Matsumoto K, Soejima H, et al. Explanation of machine learning models using shapley additive explanation and application for real data in hospital. *Computer Methods and Programs in Biomedicine* 2022;214:106584.

50. Slack D, Hilgard S, Jia E, et al. Fooling lime and shap: Adversarial attacks on post hoc explanation methods. In: Editor, editor^editors. Book Fooling lime and shap: Adversarial attacks on post hoc explanation methods. New York, NY, USA: Association for Computing Machinery; 2020. pp. 180–186.

51. Tsai CJ, Hofstede TM, Sturgis EM, et al. Osteoradionecrosis and radiation dose to the mandible in patients with oropharyngeal cancer. *International journal of radiation oncology, biology, physics* 2013;85:415–20.

52. Group MAHaNCSW. Dose-volume correlates of mandibular osteoradionecrosis in oropharynx cancer patients receiving intensity-modulated radiotherapy: Results from a case-matched comparison. *Radiotherapy and oncology : journal of the European Society for Therapeutic Radiology and Oncology* 2017;124:232–239.

53. Zhang W, Zhang X, Yang P, et al. Intensity-modulated proton therapy and osteoradionecrosis in oropharyngeal cancer. *Radiotherapy and oncology : journal of the European Society for Therapeutic Radiology and Oncology* 2017;123:401-405.
54. van Dijk LV, Abusaif AA, Rigert J, et al. Normal tissue complication probability (ntcp) prediction model for osteoradionecrosis of the mandible in patients with head and neck cancer after radiation therapy: Large-scale observational cohort. *International journal of radiation oncology, biology, physics* 2021;111:549-558.
55. Yang Y, Muller OM, Shiraishi S, et al. Empirical relative biological effectiveness (rbe) for mandible osteoradionecrosis (orn) in head and neck cancer patients treated with pencil-beam-scanning proton therapy (pbspt): A retrospective, case-matched cohort study. *Front Oncol* 2022;12:843175.